Direct Evidence of Phosphorus-Defect Complexes in *n*-Type Amorphous Silicon and Hydrogenated Amorphous Silicon

Mihail P. Petkov, Marc H. Weber, and Kelvin G. Lynn

Department of Physics, Washington State University, Pullman, Washington 99164-2814

Richard S. Crandall

National Renewable Energy Laboratory, 1617 Cole Boulevard, Golden, Colorado 80401-3393

Vinita J. Ghosh

Department of Applied Science, Brookhaven National Laboratory, Upton, New York 11973
(Received 25 November 1998)

We use positron annihilation spectroscopy (PAS) to identify the phosphorus-defect complex ($^*D^-$) in *n*-type hydrogenated amorphous Si (*a*-Si:H). The positrons are attracted and localized at the small open volume associated with the dangling bond defects. The radiation detected after annihilation gives a characteristic P signature, regarded as a $^*D^-$ "fingerprint." Additional evidence is obtained from a comparison to P-implanted amorphized Si, as well as from theoretical calculations. This work lays the foundation for PAS studies of impurity-defect related processes in *a*-Si:H. [S0031-9007(99)09089-4]

The electronic properties of hydrogenated amorphous Si (*a*-Si:H) devices, such as thin film transistors and solar cells, are controlled by states in the band gap [1], dominated by the amphoteric Si dangling bond (D) [2]. Depending on the number of electrons occupying a dangling bond (0, 1, or 2), the charge of D can be positive (D^+), neutral (D^0), or negative (D^-). These are the prevailing deep-level defects in *p*-type, intrinsic, and *n*-type *a*-Si:H, respectively. Because of the low formation energy of these defects, doping efficiency is low. Charged dangling bonds form at the expense of band edge electrons or holes. Although this is understood on theoretical grounds [3] there is no clear theoretical or experimental evidence whether the D defects pair with dopant atoms, although there are many cases of dopant/defect pairing in crystals. It was postulated, on the basis of capacitance [4] and electron spin resonance measurements [5], that an isolated D^- and a P-D^- complex ($^*D^-$) can exist in *n*-type (P doped) *a*-Si:H. However, a clear identification of the $^*D^-$, which would prompt further experimental and theoretical work and lead to a better understanding of *a*-Si:H, was not firmly established.

In this Letter, we use positron annihilation spectroscopy (PAS) to achieve the first *direct* identification of $^*D^-$. PAS has been established as a nondestructive materials characterization tool [6,7], with sensitivity to open-volume defects, spanning over wide ranges of size and concentration [8]. The method is based on the propensity of positrons, during their thermal diffusion, to "seek" and become localized at the open volume at dangling bond defects [9]. The electronic information about the surrounding environment is imprinted on the radiation produced upon annihilation with an electron. Variable-energy positron beams enable depth profiling of samples by controlling the positron implantation depth, thus making PAS ideally suitable for studying thin *a*-Si:H films and devices [9].

Conventional Doppler broadening (DB) PAS was first used to distinguish between the D^0 and D^- signatures in various *a*-Si:H alloys, and their spatial distribution in a *p*-*i*-*n* device was profiled [9]. DB, however, is mostly sensitive to the low-momentum part (<1 a.u.) of the annihilation spectrum. The higher-momentum components, which contain the differences between D^- and $^*D^-$, are obscured by the background. Our attempts to detect fine structure at large momenta (due to annihilation with core electrons) in ratios of DB spectra were unsuccessful, indicating that D^- and $^*D^-$ are indistinguishable in conventional DB experiments. To distinguish between these two defects we seek the P "fingerprint" in the annihilation spectrum of *localized* positrons, in which case a small fraction of the positron wave function overlaps with the core electrons from the nearest-neighbor atoms, and vanishes exponentially at larger distances [6].

For this end, we use coincidence PAS (CoPAS) [10], based on the analysis of coincidence DB events, registered by two energy-sensitive detectors. The energy condition $E = 2m_0c^2$ (the rest mass of the annihilating particles) is enforced to ensure the detection of the red- and blueshifted photons of the same annihilation event, resulting in a significant enhancement of the peak-to-background ratio [10]. Thus, as opposed to DB, CoPAS enables the investigation of the high-momentum contribution due to positrons annihilating with core electrons.

We exploit the elemental specificity of the P and Si atomic structures in CoPAS to distinguish between the D^- and $^*D^-$ in *a*-Si:H. The characteristic P fingerprints in the annihilation radiation are observed experimentally in *n*-type *a*-Si:H and *a*-Si, and identified by theoretical calculations.

Although we clearly distinguish between the D^- and $^*D^-$, we must stress that we obtain no information as to the bonding of the P. It could be threefold coordinated (P_3^0), the majority of the P or fourfold coordinated (P_4^+). An isolated P_3^0 in a defect-free environment or a P_4^+/D^- pair would both appear as neutral entities to the positron, whereas the P_3^0/D^- or $^*D^-$ present a large Coulomb trapping center giving a significantly larger specific trapping rate, due to its negative charge [11], than the neutral centers. Examples for such competition between neutral and negatively charged defects in other materials can be found in the literature [12]. Therefore, the positron annihilation in n-type a-Si:H and a-Si originates from the negative dangling bond defects, D^- or $^*D^-$.

a-Si:H alloys were produced at the National Renewable Energy Laboratory by glow-discharge (GD) chemical vapor deposition. Intrinsic (TP29) and n-type (S940429-#109) samples were deposited at 250 °C substrate temperature. Typically, GD a-Si:H contains about 9 at. % H as measured by infrared absorption. The n-type material was produced by the decomposition of a mixture of silane and phosphine, resulting in a P concentration of approximately 900 ppm in the a-Si:H alloy. The thicknesses of the intrinsic and the n-doped films were 1600 and 580 nm, respectively, measured by a profilometer.

Samples prepared by ion implantation were used for comparison with a-Si:H. A reference amorphous Si (a-Si) was obtained by room temperature 200 keV ^{29}Si$^+$ implantation of n-type float-zone (FZ) single crystal Si(100) to a fluence of 1×10^{16} cm^{-2}. The ^{29}Si isotope was chosen over ^{28}Si in order to avoid accidental nitrogen contamination of the sample. The a-Si structure was subsequently relaxed at 500 °C for 2 h. The P-rich a-Si sample was produced by ^{31}P$^+$ implantation (200 keV, 1.7×10^{15} cm^{-2}) of FZ Si(100), preceded by ^{29}S$^+$ implantation (150 keV, 1×10^{15} cm^{-2}), to enhance the degree of amorphization. This sample was not subjected to a structural relaxation.

A coincidence system was constructed with two high-efficiency high-purity Ge detectors with a combined resolution of 2.12 keV (at 514 keV, ^{85}Sr) for measuring the total Doppler shift, $2\Delta E = p_\parallel c$, due to the longitudinal component of the electron momentum. A tunable monoenergetic positron beam, providing $\sim10^5$ e^+/s, was used to probe the samples as a function of depth. The energy for CoPAS experiments was chosen so that the interior of the amorphous material was probed. Spectra of $(30-40) \times 10^6$ counts and $\sim100 \times 10^6$ counts were acquired for each of the a-Si and a-Si:H samples, respectively.

The measured by CoPAS annihilation probability densities of the intrinsic and n-type a-Si:H and a-Si are very similar (Fig. 1), showing small differences at high-momentum annihilation. Although a typical spectrum extends to ±12 a.u., we focus on the $|p_\parallel| < 3.5$ a.u. region, for which the experimental error is sufficiently small with respect to the observed differences. To enhance the

fine structure contained in the spectra, ratios of *pairs* of spectra of P-containing material and undoped material are produced, taking special care to ensure the similarity of sample preparation. We compare the ratios of the experimental spectra of (1) P doped versus intrinsic a-Si:H; (2) P-implanted versus ^{29}Si-amorphized a-Si; theoretically calculated ratios for (3) hypothetical P crystal versus Si crystal (c-Si); (4) P-vacancy complex versus vacancy in c-Si; (5) P-D^0 complex versus D^0 in a-Si:H with P at the nearest Si site.

Ratios of the doped to undoped CoPAS spectra of a-Si and a-Si:H pair samples are shown in Fig. 2(a) (a-Si—crosses; a-Si:H—solid circles). The experimental data are smoothed with a Gaussian whose width corresponds to the detector resolution. Because of the extra trapped electron, the low-momentum annihilation at D^- (or $^*D^-$) is enhanced in comparison to D^0 [9], giving a ratio larger than unity at $p_\parallel = 0$ a.u. Closer inspection shows different widths of the low-momentum peaks for a-Si and a-Si:H. The narrower peak for the a-Si ratio is an indication of smaller differences between the electron momentum distributions within the defects of the P- and Si-implanted material, as compared to the P-doped and the intrinsic a-Si:H. This can be caused by a larger open volume of the defects in the implanted Si, or by the H in a-Si:H, modifying the distribution of the localized positron wave function.

Well-pronounced peaks at $p_\parallel = \pm1.40$ a.u. (vertical lines) appear in the a-Si and a-Si:H curves. A second set of peaks at $p_\parallel \cong \pm3$ a.u. can be seen in the ratio of the ion-implanted samples, but are not present in the a-Si:H ratio. Further studies are needed to reveal these minor details. The statistical error at $p_\parallel = \pm1.40$ a.u. before the smoothing is 0.7% for the a-Si ratio and approximately the symbol size for the a-Si:H. The strong peaks at this value of $p_\parallel$ are clearly revealed after subtraction of the broad central component, approximated
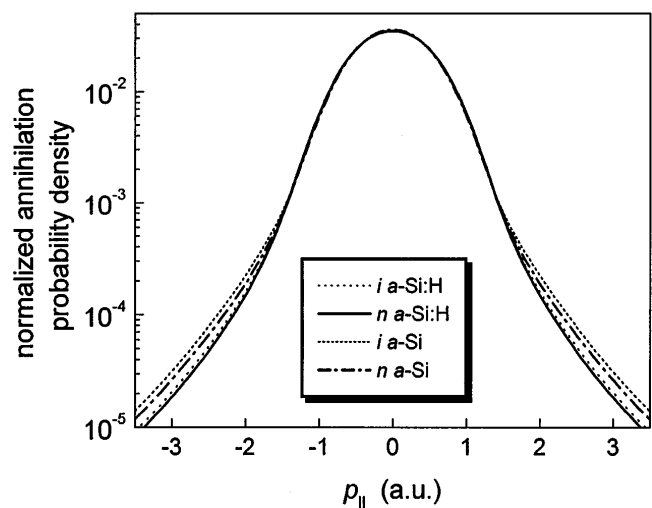

FIG. 1. Experimental CoPAS spectra of n- and i-type a-Si and a-Si:H (limited to $|p_\parallel| < 3.5$ a.u.).
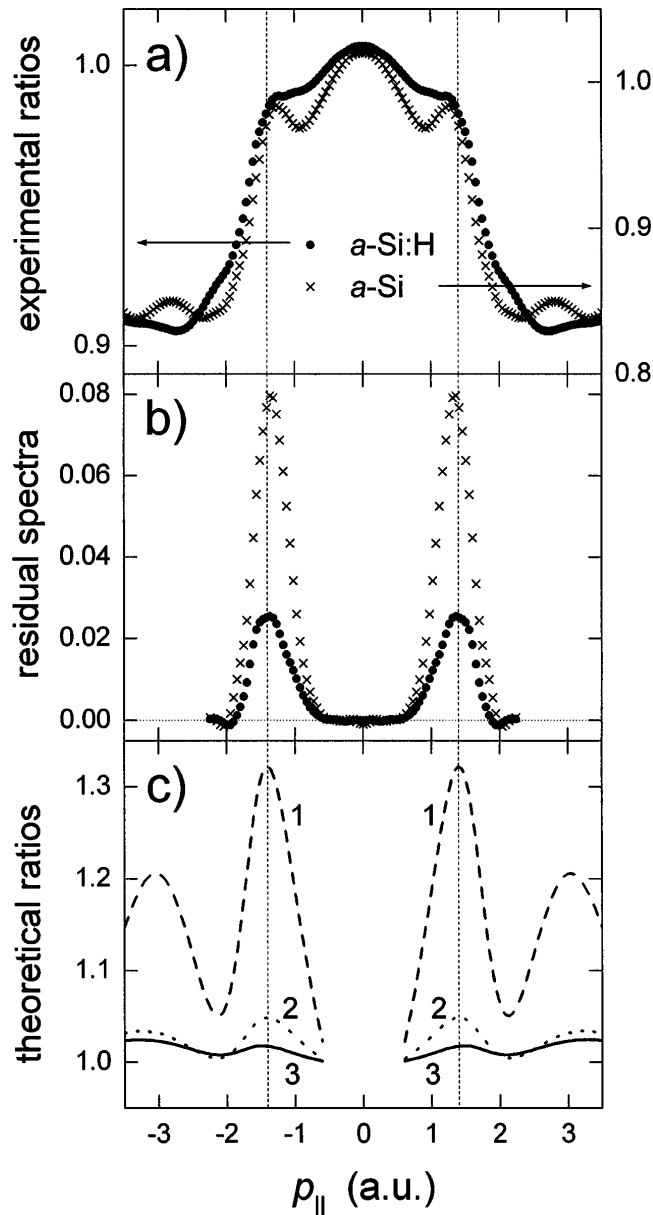
FIG. 2.   (a) Experimental ratios of doped-to-undoped a-Si:H (solid circles) and a-Si (crosses), with the arrows pointing towards the respective scale; (b) residual spectrum after subtracting a central Gaussian component from the curves in (a) (same symbols); (c) theoretical calculations of the following ratios: (1) P on Si lattice versus Si crystal (dashed line); (2) P-vacancy complex versus vacancy in c-Si (dotted line); (3) $^*D^0$ versus D^0 in a-Si:H (solid line).

by a Gaussian [Fig. 2(b), same symbols]. As a first-order approximation, this approach takes care of the slope of the ratio curve at $p_\parallel = \pm 1.40$ a.u.

We use the P-implanted amorphized Si to shed light on the nature of the strong features at $p_\parallel = \pm 1.40$ a.u. It is well established that P binds very efficiently to vacancylike defects in Si [13]. Thus, the large and compatible P and D densities at the probed depth provide a strong annihilation signal from P-decorated defects. Well-defined features, due to the annihilation of positrons

with the phosphorus L-shell electrons, can then be seen in comparison to self-implanted a-Si, as in Fig. 2(a).

In light of the findings of Ref. [10], elements other than P would create features in the ratio curves at different values of $p_\parallel$. The clear similarities in the structure of the a-Si and a-Si:H ratio data at $p_\parallel = \pm 1.40$ a.u. bring a firm experimental support for the recognition of the $^*D^-$ defects in the n-type a-Si:H. Nevertheless, the peaks at $p = \pm 1.40$ a.u. are not conclusively identified as P fingerprints without theoretical support.

A rough estimate of the expected Doppler shift caused by the L-shell electrons of P can be made using the Virial theorem to approximate the electron kinetic energy by its binding energy. The obtained value (1.58 a.u.) is in a fair agreement with the measured $p_\parallel = 1.40$ a.u. Since Ref. [14] shows that such calculations consistently overestimate the magnitude of the experimentally observed Doppler shifts, we perform detailed theoretical calculations [15], to obtain the momentum distribution for a Si crystal, and for a hypothetical P crystal, created by replacing each Si atom of the diamondlike lattice with a P atom. Similar atomic superposition model calculations have been compared with experimental data [12]. They reproduce qualitatively all experimental features, though the quantitative differences can be as large as a factor of 2.

The calculated momentum distribution densities were convoluted with the experimental sampling function (detector resolution), and their ratio is shown in Fig. 2(c) (dashed line). The inadequate values for small $|p_\parallel|$ (less than ~ 1 a.u.) are unimportant for our discussion and are omitted from all calculated ratios. Although such a P crystal does not exist, it serves to establish the P fingerprint peaks in the ratio curve of ± 1.40 a.u. and approximately ± 3 a.u. The positions of the peaks at $p_\parallel = \pm 1.40$ a.u. (Fig. 2, vertical lines) are in excellent agreement with the experimentally observed ones in the a-Si and a-Si:H ratios. Moreover, the $p_\parallel \approx \pm 3$ a.u. peaks in the a-Si data are also predicted by the theory.

The same calculations were repeated to obtain the momentum distribution spectra of positrons annihilating at a Si vacancy (V) and a P-decorated Si vacancy (P-V) in c-Si. The ratio P-V vs V is also shown in Fig. 2(c) (dotted line). The characteristic P-related peaks appear at the same value of the longitudinal momentum, though the height of the peaks decreased. The peak positions are characteristic of the chemical structure, and the peak height is determined by the crystal and defect geometry [16].

The momentum distribution calculations were extended to a-Si:H, using supercells with Si and H positions obtained by molecular dynamics simulations [17]. By replacing a Si with a P atom in the immediate vicinity of the defect, thus simulating $^*D^0$, the momentum distribution ratios of $^*D^0$ vs D^0 were calculated for two supercells. The addition of an extra charge as in $^*D^-$ requires additional assumptions on the momentum distribution of the extra electron, and it is not considered at this time. Nevertheless, we can still distinguish between $^*D^0$ and

D^0. Their ratio is shown in Fig. 2(c) (solid line). We investigated the sensitivity of the calculations to the size of the open volume at $^*D^0$, by adding an extra vacancy to the $^*D^0$ site, thus forming $^*D^0 + V$, for which the ratio to D^0 was recalculated. The higher momentum region >3 a.u. is sensitive to the open volume. Since our experimental error in this region is large, we cannot distinguish these effects.

The theoretical calculations are in excellent agreement with the experimental data and achieve the positive identification of the $^*D^-$ complex. The fingerprints of the P L-shell annihilation at $p_\| = \pm 1.40$ a.u. appear in all ratios of "n-to-i" type materials with different signal strengths. Furthermore, the smaller peaks at $p_\| \approx \pm 3$ a.u., seen in the experimental a-Si ratio, are also evident in the theoretical calculations. The intensity of a given electron annihilation signal depends on the overlap between the positron and the electron wave functions and the open-volume size of the defect. As the open volume increases, the core-electron annihilation diminishes. This is reflected in the different peak heights for the different sets of experimental and theoretical ratio curves. The detection of the second peak (if present) at $p_\| \approx \pm 3$ a.u. in the a-Si:H data, however, depends strongly on the structural configuration of the defect, as indicated by the calculated $^*D^0 + V$ versus D^0 ratio.

As $^*D^-$ and D^- localize positrons identically, the respective contributions to the annihilation spectrum scale with their respective concentrations. A quantitative analysis of the $D^-/^*D^-$ concentration ratio in n–type a-Si:H cannot be performed at this stage because of the lack of $^*D^-$ and D^- experimental reference. The atomic superposition calculations cannot provide additional insights, because of the strong dependence on the input structure from molecular dynamic simulations. Nevertheless, we argue that $^*D^-$ is the dominant defect based on the following facts. First, contrary to doping of crystalline Si, a sizable amount of the P atoms in a heavily doped (5×10^{19} cm^{-3}) a-Si:H remains threefold coordinated [3,4], accounting for a density compatible to that of the dangling bond defects (5×10^{18} cm^{-3}). Second, molecular dynamics simulations [17] show the presence of open volume at the threefold coordinated D defects. And third, it is well established that P atoms bind very efficiently to vacancylike defects in Si [13]. Therefore, it is probable to find P atoms bound to the open volume at D^-, thus forming $^*D^-$, and less likely existing as an isolated P_3^0 configuration.

In conclusion, here we positively identified the P fingerprint in the ratio of Doppler spectra of positron annihilation in n- vs i-type a-Si:H by comparison to theoretical calculations and samples prepared by (P and Si) ion beam implantation. We argue that the D^- and $^*D^-$ defects are indistinguishable in the process of the localization of the positron wave function, however their annihilation signatures differ by the contribution from the phosphorus L-shell electrons in the case of $^*D^-$. This is the first direct evidence of this defect complex in a-Si:H. We show that the $^*D^-$ is the dominant deep-level defect in heavily doped n-type a-Si:H. Further progress in the characterization of the impurity-defect complexes in a-Si:H, as well as in the development of detailed theoretical models can be achieved by another PAS technique—2-dimensional angular correlation of the annihilation radiation.

[1] R. S. Crandall and Q. Wang, Conf. Rec. IEEE Photovoltaic Spec. Conf. **25**, 1117 (1996).

[2] R. A. Street, *Hydrogenated Amorphous Silicon* (Cambridge University Press, Cambridge, England, 1991).

[3] R. A. Street, Phys. Rev. Lett. **49**, 1187 (1982).

[4] H. Okushi, S. Yamazaki, and K. Tanaka, J. Non-Cryst. Solids **141**, 176 (1992).

[5] H. Okushi and K. Tanaka, Philos. Mag. Lett. B **55**, 135 (1987).

[6] P. Schultz and K. G. Lynn, Rev. Mod. Phys. **60**, 701 (1988).

[7] M. J. Puska and R. M. Niemenen, Rev. Mod. Phys. **66**, 841 (1994).

[8] http://www-phys.llnl.gov/H_Div/Positrons/PositronMaterials.html

[9] M. P. Petkov, T. Marek, P. Asoka-Kumar, K. G. Lynn, R. S. Crandall, and A. H. Mahan, Appl. Phys. Lett. **73**, 99 (1998).

[10] P. Asoka-Kumar, M. Alatalo, V. J. Ghosh, A. C. Kruseman, B. Nielsen, and K. G. Lynn, Phys. Rev. Lett. **77**, 2097 (1996).

[11] For example, a neutral vacancy in Si crystal has a 5 times smaller positron trapping rate than a negatively charged vacancy. See P. Mascher, S. Dannefaer, and D. Kerr, Phys. Rev. B **40**, 11 764 (1989).

[12] T. C. Leung, P. Asoka-Kumar, B. Nielsen, and K. G. Lynn, J. Appl. Phys. **73**, 168 (1993).

[13] J. Mäkinen, P. Hautojärvi, and C. Corbel, J. Phys. Condens. Matter **4**, 5137 (1992).

[14] U. Myler and P. J. Simpson, Phys. Rev. B **56**, 14 303 (1997).

[15] V. J. Ghosh, M. Alatalo, P. Asoka-Kumar, K. G. Lynn, and A. C. Kruseman, Appl. Surf. Sci. **116**, 278 (1997).

[16] M. Alatalo, P. Asoka-Kumar, V. J. Ghosh, B. Nielsen, K. G. Lynn, A. C. Kruseman, A. Van Veen, and M. J. Puska, J. Phys. Chem. Solids **59**, 55 (1998).

[17] Q. Li and R. Biswas, Phys. Rev. B **52**, 10 705 (1995).